Study of the Ca$_x$Eu$_{1-x}$FeO$_{3-y}$ System

Bull. Korean Chem. Soc. **1994**, Vol. 15, No. 7 541

1966, *88*, 5121.

2. Collman, J. P. *Acc. Chem. Res.* **1975**, *8*, 342.

3. Darensbourg, M. Y.; Darensbourg, D. J.; Drew, D. A.; Burns, D. *J. Am. Chem. Soc.* **1976**, *98*, 3127.

4. Moro, A.; Foa, M.; Cassar, L. *J. Organomet. Chem.* **1980**, *212*, c68.

5. (a) Darensbourg, M. Y.; Jimenez, P.; Sackett, J. R.; Hankel, J. M.; Kump, R. L. *J. Am. Chem. Soc.* **1982**, *104*, 1521; (b) Darensbourg, M. Y.; Jimenez, P.; Sackett, J. R. *J. Organomet. Chem.* **1980**, *202*, c68.

6. Winston, P. L.; Bergman, R. G. *J. Am. Chem. Soc.* **1979**, *101*, 2055.

7. Darensbourg, M. Y. *Progress in Inorganic Chemistry*; John Wiley & Sons, Inc.: New York, U. S. A., 1985; Vol. 33, p 222.

8. Park, Y. K.; Han, I. S.; Huh, T. S. *Bull. Kor. Chem. Soc.* **1990**, *11*, 221.

9. Park, Y. K.; Kim, S. J.; Kim, J. H.; Han, I. S.; Lee, C. H.; Choi, H. S. *J. Organomet. Chem.* **1991**, *408*, 193.

10. Anders, U.; Graham, W. A. *J. Am. Chem. Soc.* **1967**, *89*, 539.

11. Arndt, L. W. Dissertation, Texas A & M Univ. **1986**.

12. Ruff, J. K. *Inorg. Chem.* **1968**, *7*, 1818.

13. Closson, R. D.; Kozikowski, J.; Coffield, T. H. *J. Org. Chem.* **1966**, *22*, 598.

14. Hayter, R. G. *J. Am. Chem. Soc.* **1966**, *88*, 4376.

Study of Nonstoichiometry and Physical Properties of the Ca$_x$Eu$_{1-x}$FeO$_{3-y}$ System

Kwon Sun Roh, Kwang Sun Ryu, Kwang Hyun Ryu, and Chul Hyun Yo

Department of Chemistry, Yonsei University, Seoul 120-749, Korea
Received January 27, 1994

A series of samples of the Ca$_x$Eu$_{1-x}$FeO$_{3-y}$ ($x=0.00$, 0.25, 0.50, 0.75, and 1.00) system has been prepared at 1,250℃ under an atmospheric air pressure. X-ray diffraction analysis of the solid solution assigns the structure of the compositions of $x=0.00$, 0.25, 0.50, and 0.75 to the orthoferrite-type orthorhombic system, and that of $x=1.00$ to the brownmillerite-type orthorhombic one. The mole ratios of Fe^{4+} ion in the solid solutions or τ values were determined by the Mohr's salt analysis and nonstoichiometric chemical formulas of the system were formulated from x, τ, and y values. From the result of the Mössbauer spectroscopy, the coordination and magnetic property of the iron ion are discussed. The electrical conductivities are measured as a function of temperature. The activation energy is minimum at the composition of $x=0.25$. The conduction mechanism can be explained by the hopping of electrons between the mixed valences of Fe^{3+} and Fe^{4+} ions.

Introduction

Perovskite-type compounds,[1-7] ABO$_3$, have been extensively studied because of their unique and applicable properties due to the mixed valence state of B ion and oxygen vacancy. The properties can be controlled by the substitution of lower valence metals such as Ca^{2+}, Sr^{2+}, and Ba^{2+} in place of higher one, Ln^{3+}, as well as the heating temperature and oxygen pressure maintained during the synthesis.

The orthoferrites[8] have the formula of RFeO$_3$ where R is rare earth metals. The ferrite has the distorted perovskite structure in which the iron environment retains essentially octahedral but an octahedral chain along a c-axis has the form of zigzagging. The degree of zigzagging is determined to a large extent by the size of R ion. The larger the R ion, the more the chain stretchs, the degree of zigzagging decreases. The substitution of larger alkaline earth metal in place of rare earth metal accelerates the phenomenon. The compositions of $x=0.50$ and 0.25 in the Sr$_x$La$_{1-x}$FeO$_{3-y}$ and Ba$_x$La$_{1-x}$FeO$_{3-y}$ systems[6,9] have the ideal cubic perovskite structure in which Fe-O-Fe angle is 180 degree. In these systems, the valence state of Fe ion changes partly from the trivalent to the tetravalent state with increasing Sr^{2+} or Ba^{2+} ion content and the electrical conductivity increases. The magnetic ordering temperature decreases with increasing x value, which is explained by the superexchange model.[10]

In the study of defect model for perovskite oxides, Roosmalen *et al.*[11] have suggested that in the SrMnO$_{3-y}$ the Mn^{3+} ions are coordinated trigonal bipyramidally and octahedrally, while the structure for SrFeO$_{3-y}$ consists of tetragonally and octahedrally coordinated iron ions. Grenier *et al.*[12] have investigated the Mössbauer resonance effect on the Ca$_{2y}$La$_{1-2y}$FeO$_{3-y}$ system in which the ratios of six and four coordinated iron ions increase with y value, while the variation of Néel temperature is not significant on the contrary, in Sr$_x$La$_{1-x}$FeO$_{3-y}$ and Ba$_x$La$_{1-x}$FeO$_{3-y}$ systems.

The CaFeO$_3$[13,14] prepared only under higher oxygen partial pressure, has the crystal structure distorted slightly from cubic system and the charge disproportionation of Fe^{4+} ion into Fe^{3+} and Fe^{5+} ions occurs at the liquid helium temperature. The CaFeO$_{2.5}$ system[15,16], however, has the brownmillerite-type orthorhombic structure in which the oxygen vacancy ordering along [101] strings occurs in every other (010) plane and a slight shift of the iron atoms in these planes

leads to a structure with alterating sheets of (FeO$_6$) octahedra and of (FeO$_4$) tetrahedra.

In the present study, the solid solutions of the Ca$_x$Eu$_{1-x}$·FeO$_{3-y}$(x=0.00, 0.25, 0.50, 0.75, and 1.00) system have been prepared and their structures are analyzed by X-ray diffraction. The amount of Fe^{4+} ion or the mixed valence state between Fe^{3+} and Fe^{4+} ions is determined by Mohr's salt titration. The nonstoichiometric chemical formula for the Ca$_x$Eu$_{1-x}$Fe$^{3+}_{1-\tau}$ Fe$_\tau$$^{4+}O_{3-y}$ system is determined. The Mössbauer resonance effect and electrical conductivity will be discussed with the nonstoichiometric compositions.

Experimental

Solid solutions for the compositions of x=0.00. 0.25, 0.50, 0.75, and 1.00 in the Ca$_x$Eu$_{1-x}$FeO$_{3-y}$ system have been prepared as followings. The starting materials such as Eu$_2$O$_3$, CaCO$_3$, and Fe(NO$_3$)$_3$·9H$_2$O were weighed and dissolved in the dilute nitric acid. The solution was evaporated over a burner flame and then the nitrates were decomposed at 800 ℃ for 4 hours. After being ground and mixed, the mixtures were heated at 1,250℃ under an atmospheric air pressure for 36 hours. The grinding and heating processes were repeated several times in order to produce homogeneous solid solution.

The solid solutions are identified by the powder X-ray diffraction analysis with a PHILIPS pw 1710 diffractometer using monochromatized CuKα (λ=1.5406 Å) radiation. Lattice parameters, reduced lattice volume of the unit cell, and crystal system for the solid solutions were determined reasonably.

The chemical analysis was carried out to determine the oxidation state of the iron ions by dissolving the samples in 0.1 N solution of Mohr's salt in the presence of HCl and titration with K$_2$Cr$_2$O$_7$ solution. The results obtained were reproducible and self-consistent. Oxygen vacancy and nonstoichiometric chemical formulas for the system were also determined.

The Mössbauer spectra were recorded at room temperature using a spectrometer consisted of a 308-channel pulse-height analyzer and a source of ^{57}Co/Rh with 14.4 KeV γ-radiation. Isomer shift, quadrupole splitting, and hyperfine field were determined relative to the spectrum of α-Fe.

Electrical conductivity measurements were carried out on the pressed and sintered pellets using four probe *d.c.* technique in the temperature range of 173 to 873 K under ambient atmosphere. Electrical conductivities were calculated by Laplume's equation.

Results and Discussion

Solid solutions with the compositions of x=0.00, 0.25, 0.50, 0.75, and 1.00 in the Ca$_x$Eu$_{1-x}$FeO$_{3-y}$ system have been prepared at 1250℃ under an atmospheric air pressure. From the result of the powder X-ray diffraction analysis for all the compositions the patterns show two crystallographically distinct phases. The compositions of x=0.00, 0.25, 0.50, and 0.75 present characteristic patterns of the orthoferrite-type orthorhombic perovskite, while the composition of x=1.00 represents the brownmillerite one without any other phase evidence.

Table 1. Lattice Parameters, Reduced Lattice Volume, and Crystal System for the Ca$_x$Eu$_{1-x}$FeO$_{3-y}$ System

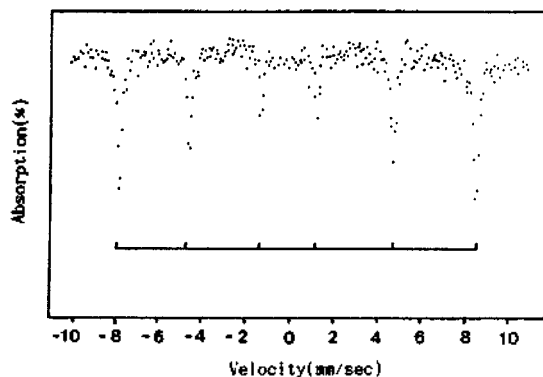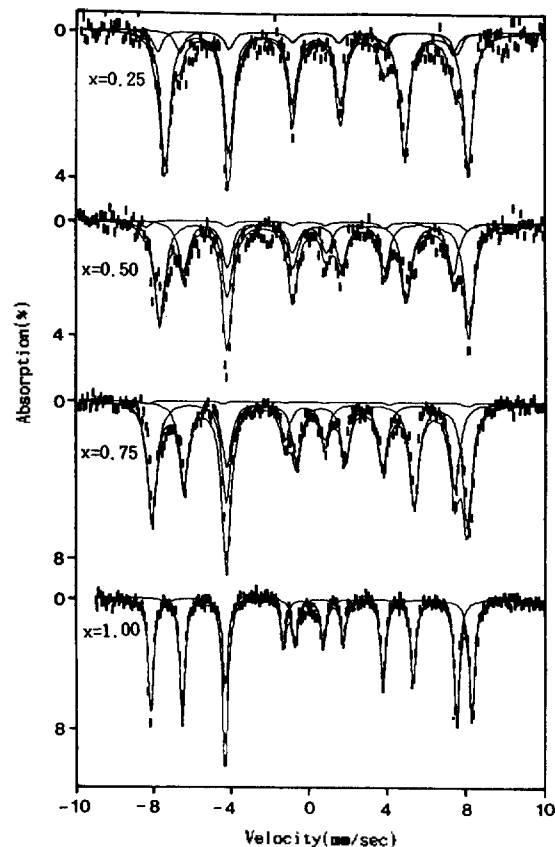| x value	Lattice parameters (Å)			Reduced lattice volume (Å^3)	Crystal system
	a	b	c		
0.00	5.338	5.564	7.648	227.2	orthorhombic
0.25	5.375	5.585	7.666	230.1	orthorhombic
0.50	5.389	5.594	7.669	231.2	orthorhombic
0.75	5.410	5.598	7.652	231.7	orthorhombic
1.00	5.432	14.76	5.607	224.7	orthorhombic
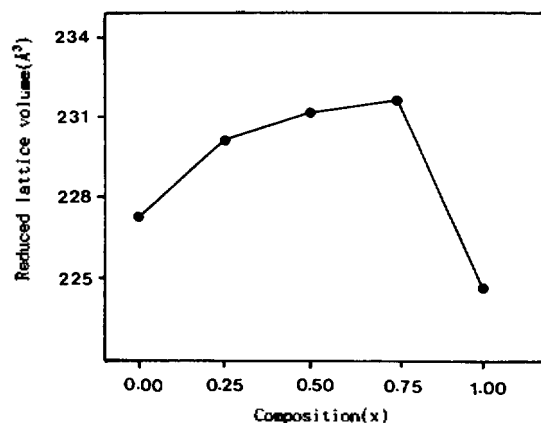
Figure 1. Plot of reduced lattice volume *vs.* x value for the Ca$_x$Eu$_{1-x}$FeO$_{3-y}$ system.

Lattice parameters, reduced lattice volume of the unit cell, and crystal system for the corresponding compositions are listed in Table 1. The unit cell volume of ABO$_3$ system is affected by three factors such as the ionic radius of the substituted ion in the A-site, the oxygen vacancy, and the mixed valence state of the B-site. As shown in Figure 1, the reduced cell volume increases with the x value in the range of 0.00≤x≤0.75. However, the volume decreases at the composition of x=1.00 where phase transition occurs. Considering the similar radii of the A-site ions and slight formation of the mixed valence state of the B-site, the oxygen vacancy results in the decreasing covalency between the iron ions, so that the effect is predominent in our system.

The mole ratio of Fe^{4+} ion or τ value, the amount of oxygen vacancy or y value, and the nonstoichiometric chemical formula corresponding to each composition are listed in Table 2. The composition of x=0.00 or EuFeO$_{3.00}$ is a stoichiometric compound and the others are all nonstoichiometric compounds. The composition of x=0.25 has the maximum τ value as shown in Figure 2. However, the τ value decreases steadily with increasing x value in the range of 0.25≤x≤1.00 in which the formation of oxygen vacancies might be easier than the formation of Fe^{4+} ion. Thus the y value increases with the x value and the ordering of the vacancies decreases the lattice energy. According to the X-ray diffraction analysis, it were found that oxygen vacancies in the compositions of the range of 0.25 ≤x≤0.75 are randomly distributed in the orthoferrite-type (2$^{\frac{1}{2}}$a$_c$×2$^{\frac{1}{2}}$a$_c$×2a$_c$) unit cell. However, the oxygen vacancy ordering occurs in the composition of x=1.00

Table 2. x, τ, y Values, and Nonstoichiometric Chemical Formula for the $Ca_xEu_{1-x}FeO_{3-y}$ System

x	τ	y	Chemicl Formula
0.00	0.00	0.00	$EuFe(II)O_{3.00}$
0.25	0.09	0.08	$Ca_{0.25}Eu_{0.75}Fe(III)_{0.91}Fe(IV)_{0.09}O_{2.92}$
0.50	0.05	0.23	$Ca_{0.50}Eu_{0.50}Fe(III)_{0.95}Fe(IV)_{0.05}O_{2.77}$
0.75	0.04	0.36	$Ca_{0.75}Eu_{0.25}Fe(III)_{0.96}Fe(IV)_{0.04}O_{2.64}$
1.00	0.00	0.50	$CaFe(III)O_{2.50}$
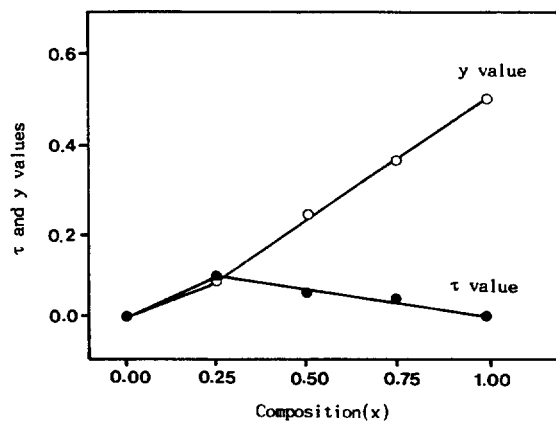
Figure 2. Plots of τ and y values *vs.* x value for the $Ca_xFu_{1-x}FeO_{3-y}$ system.

Figure 3. Mössbauer spectrum of the $EuFeO_{3.00}$ system.

along [101] strings in every other (010) plane which results in alternating sheets of (FeO_6) octahedra and of (FeO_4) tetrahedra.

The Mössbauer spectra at room temperature for all the compositions are shown in Figures 3-4. The Mössbauer parameters for all the compositions are listed in Table 3. The spectrum for the composition of $x = 0.00$ or $EuFeO_{3.00}$ consists of a series of six lines split under internal magnetic field, which is characteristic of the magnetic ordering below the Néel temperature. The isomer shift, 0.237 mm/sec, and the hyperfine field, 509 KOe, are consistent with Zeeman splitting of Fe^{3+} ion at the octahedral site. The large quadrupole splitting, 0.121 mm/sec. reflects the zigzagging form of the octahedral axis along a c-axis.

The Mössbauer spectra for the compositions of $x = 0.25$,

Figure 4. Mössbauer spectra of the compositions of $x = 0.25$, 0.50, 0.75, and 1.00.

Table 3. Mössbauer Parameters* for the $Ca_xEu_{1-x}FeO_{3-y}$ System

x value	Ion state	Coordinated site	δ (mm/sec)	ΔEq (mm/sec)	Hn (kOe)
0.00	Fe^{3+}	Oh	0.237	0.121	509
0.25	Fe^{3+}	Oh	0.363	−0.003	485
	Fe^{3+}	Td	0.181	0.474	438
	Fe^{4+}	Oh	−0.074	0.072	480
0.50	Fe^{3+}	Oh	0.338	−0.369	493
	Fe^{3+}	Td	0.180	0.616	431
	Fe^{4+}	Oh	−0.110	0.019	514
0.75	Fe^{3+}	Oh	0.302	−0.561	503
	Fe^{3+}	Td	0.150	0.733	433
	Fe^{4+}	Oh	−0.135	0.046	511
1.00	Fe^{3+}	Oh	0.253	−0.227	513
	Fe^{3+}	Td	0.114	0.377	438

*δ: isomer shift, ΔEq: quadrupole splitting, and Hn: hyperfine field.

0.50, and 0.75 can be fitted by using three series of sextets as shown in Figure 4. From the result of Mohr salt analysis, it is found out that there exist the mixed valence state between the Fe^{3+} and Fe^{4+} ions and the high anionic vacancy concentration in each composition. The isomer shift of the first sextet with the largest intensity is consistent with that
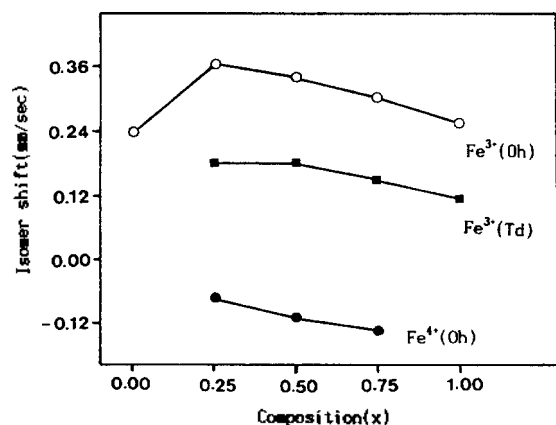
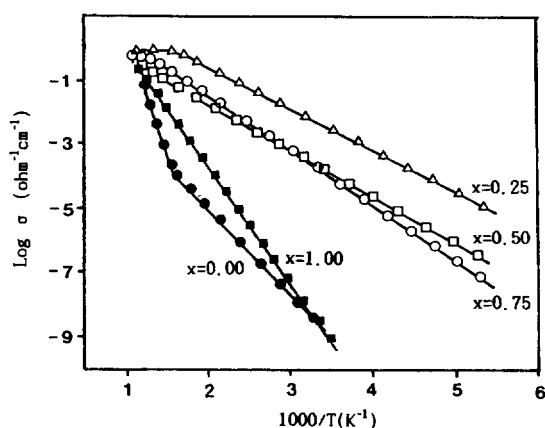**Figure 5.** Isomer shift *vs.* *x* value for the $Ca_xEu_{1-x}FeO_{3-y}$ system.

Figure 6. Plots of Log σ *vs.* 1000/T for the $Ca_xEu_{1-x}FeO_{3-y}$ system.

Table 4. Activation Energy of the Electrical Conductivity for the $Ca_xEu_{1-x}FeO_{3-y}$ System

x value	Activation energy (eV)
0.00	0.55 (173 K-663 K)
	1.58 (663 K-873 K)
0.25	0.26
0.50	0.29
0.75	0.34
1.00	0.71

of Fe^{3+} ion at the octadedral site. The intermediate isomer shift of the second sextet, which has the increasing intensity with *x* value, allows us to attribute it to the Fe^{3+} ion at the tetrahedral site.[7] The negative isomer shift corresponds to that of Fe^{4+} ion at the octahedral site. Mössbauer spectrum for the composition of $x=1.00$ shows two series of six lines with the similar intensity, which is due to the similar concentration of two different Fe^{3+} ions located in the octahedral and tetradral sites. The isomer shift and hyperfine field of the Fe^{3+} ion at the octahedral site are 0.253 mm/sec and 513 KOe, respectively. Those of the Fe^{3+} ion at the tetrahedral site are also 0.114 mm/sec and 438 KOe. In fact, such a result might be expected in the brownmillerite-type orthorhombic system.

The plots of the isomer shifts for the differently coordinated Fe ions as a function of *x* value are shown in Figure 5. The isomer shifts are in the order of $Fe^{3+}(Oh)>Fe^{3+}(Td)>Fe^{4+}(Oh)$, which is due to increasing electron density at the nucleus. The isomer shift of Fe^{3+} ion at octahedral site is maximum at the composition of $x=0.25$ and decreases with the increasing *x* value. The isomer shifts of Fe^{3-} ion at tetrahedral site and Fe^{4+} ion at octahedral one decrease with the increasing *x* value. It is ascribed to the fact that the Fe^{4+} ion with higher charge and smaller ionic radius attracts neighboring oxygen ions and the covalency between

the Fe^{4+} and oxygen ions becomes significant. Reversely, the Fe^{3+} ion neighboring Fe^{4+} ion has the decreasing covalency with oxygen ions, which results in increasing isomer shift of Fe^{3+} ion. However, since the amount of Fe^{4+} ion is maximum at the composition of $x=0.25$ and decreases in the range of $0.25 \leq x \leq 0.75$, the isomer shift of the Fe^{3+} ion decreases in the above range. Since the quadrupole splitting results from the electrical field gradient at the nucleus of the iron ion, it reflects asymmetry of coordinating oxygen ligands around the ion. The quadrupole splitting of the iron ion at tetrahedral site is larger than that of octahedral one as shown in Table 3, which is due to a slight shift of the nucleus from oxygen vacancy. The quadrupole splitting of the Fe^{3+} ion at octahedral site is abnormally small at the composition of $x=0.25$. It reflects the smallest amount of oxygen vacancies with increasing regular arrangement of oxygen ions.

The electrial conductivity measurement has been carried out in the temperature range of 173-873 K under the air pressure as shown in Figure 6. The activation energies of the conductivity are listed in Table 4 for all the compositions in the given temperature ranges. For all the compositions, the conductivity increases with increasing temperature as a semiconductor behavior. The compositions of the $x=0.00$ and $x=1.00$ without the Fe^{4+} ion has lower conductivity than those of the compositons of $x=0.25$, 0.50, and 0.75 with the Fe^{4+} ions. The slope change of the Arrhenius plot of conductivity for the composition of $x=0.00$ occurs at about 663 K. This point is agree with the magnetic ordering one at 662 K reported by Eibschütz.[17] The magnetic ordering temperature for the compositions of $x=0.25$ to 1.00 is not detected. The compositon of $x=0.25$ has the largest conductivity in the ferrites containing Fe^{4+} ion, which is consistent with the maximum amount of Fe^{4+} ion in the composition. The activation energy of the conductivity has been varied with an opposite way to the τ value as shown in Tables 2 and 4. The mixed valence state between Fe^{3+} and Fe^{4+} ions leads to high conductivity.

In the study of the $La_{1-x}Sr_xCoO_{3-y}$ perovskite, Burren *et al.*[18] have suggested that the expression of the Seebeck coefficient in a small polaron hopping model is very suitable for calculating the hole concentration of the system. This suggestion indicates that the hopping model can be also used for other perovskites oxides. As like the similar behavior of the $La_{1-x}Sr_xCoO_{3-y}$ perovskite in which the conduction depends mainly on the Fe^{4+} ion, the conduction mechanism of our system should be represented by the hopping model of the conduction electrons in the mixed valence state be-

tween Fe^{3+} and Fe^{4+} ions.

References

1. Yo, C. H.; Lee, E. S.; Pyun, M. S. *J. Solid State Chem.* 1988, *73*, 411.
2. Yo. C. H.; Roh, K. S.; Lee, S. J.; Kim, K. H.; Oh, E. J. *J. Kor. Chem. Soc.* 199, *35*(3), 211.
3. Ryu, K. H.; Roh, K. S.; Lee, S. J.; Yo, C. H. *J. Solid State Chem.* 1993, *105*, 550.
4. Rodriguez, J.; Fontcuberta, J.; Longworth, G.; Vallet-Regí M.; González-Calbet, J. M. *J. Solid State Chem.* 1988, *73*, 57.
5. Buffat, B.; Demazeau, G.; Pouchard, M.; Dance, J. M.; Hagenmuller, P. *J. Solid State Chem.* 1983, *50*, 30.
6. Parras, M.; Vallet-Regí M.; González-Calbet, J. M.; Allar-rio-Franco, M.; Grenier, J. C. *J. Solid State Chem.* 1988, *74*, 110.
7. Wattiaux, A.; Grenier, J. C.; Pouchard, M.; Hagenmuller, P. *J. Electrochem. Soc.* 1987, *134*(7), 1714.
8. Lee, S. J., thesis, Ph. D. 1992.
9. Takano, M.; Kawachi, J.; Nakanishi, J.; Takeda, Y. *J. Solid State Chem.* 1981, *39*, 75.
10. Racah, P. M.; Goodenough, J. B. *J. Appl. Phys.* 1968, *39*, 1209.
11. Roosmalen, J. A. M. V.; Cordfunke, E. H. P. *J. Solid State Chem.* 1991, *93*, 212.
12. Grenier, J. C.; Fournés, L.; Pouchard, M.; Hagenmuller, P. *Mat. Res. Bll.* 1982, *17*, 55.
13. Gibb, T. C.; Battle, P. D.; Bollen, S. K.; Whitehead, R. J. *J. Mater. Chem.* 1992, *2*(1), 111.
14. Gibb. T. C. *J. Chem. Soc. Dalton Trans.* 1985, 1455.
15. Matsuo M.; Gibb, T. C. *J. Solid State Chem.* 1990, *88*, 485.
16. Takano, M.; Olita, T.; Nakayama, N.; Bando, Y.; Takeda, Y.; Yamamoto, O.; Goodenough, J. B. *J. Solid State Chem.* 1998, *73*, 140.
17. Eibschütz, M.; Shtrikman, S.; Takeda, Y. *Phys. Rev.* 1967, *156*(2), 562.
18. Burren, P. R. V.; Dewit, J. H. W. *J. Electrochem. Soc.* 1979, *126*, 1817.

Electronic Structure and Properties of High-T_c Substituted YBCO Superconductors: II. MO Calculations on Charged Cluster Models Relating to High-T_c Se-Substituted YBCO Superconductors

Kee Hag Lee*, Wang Ro Lee, and U-Sung Choi**

Department of Chemistry and
**Department of Electronic Material Engineering, WonKwang University, Iri 570-749, Korea
Received February 7, 19994

Using the extended Hückel molecular orbital method in connection with the tight binding model, we have studied electronic structure and related properties of the charged cluster models relating to superconducting $YBa_2Cu_3O_{7-x}$ crystals in which O-atoms in regular sites were selectively replaced with Se atoms. In analogy to the isomorphism problem with molecules, we discuss all possible combinations of Se-substitutions in O-sites with one, two, and four Se atoms. The calculations are carried out within charged cluster models for analogues of YBa-copper oxide. Our results suggest that the electronic structure of the symmetrically Se-substituted or Se-added compound is closer to that of the YBCO superconducting compound than that obtained from the unsymmetrical substitution. This applies in particular if O is replaced with Se around the Cu(1) site. Symmetrical substitutions in the CuO_2 layers give rise to large variations in the electronic structure of $YBa_2Cu_3O_7$. This is consistent with the fact that superconductivity is very sensitive to the electronic population of the CuO_2 layers.

Introduction

Since the discovery of copper oxide with transition temperature T_c near 93 K in the Y-Ba-Cu-O systems,[1] a number of attempts have been made to increase T_c for High-T_c superconductors. These[2-4] and other studies[5-10] have stimulated research to modify the chemical composition by isomorphic replacement of the element in order to raise T_c and to examine the mechanism of High-T_c superconductivity by subs-

tituting various elements in the $YBa_2Cu_3O_{7-y}$ compound. It was found that yttrium could be replaced with rare-earth metals[2] with no increase, *i.e.* enhancement, of critical temperature. Similarly, when barium is replaced with other alkaline earth metals,[3] the overall trend is toward a continuous decrease of T_c. Also, 3d transition-metal substitution[4] for Cu gives rise to a diminution of T_c as the doping is increased.

In the $YBa_2Cu_3O_{7-y}$ system, the superconductive properties are strongly correlated with its oxygen content.[5] Several pa-